

# **PRESTRESS LOSSES AND THE ESTIMATION OF LONG-TERM DEFLECTIONS AND CAMBER IN PRESTRESSED CONCRETE BRIDGES**

Hema Jayaseelan, and Bruce W. Russell

## **INTRODUCTION**

The vast majority of new highway bridges built in the US are made from precast, prestressed concrete girders. In the last two decades, the widespread use of High Performance Concrete (HPC) has permitted longer spans, increased girder spacings and allowed shallower depths. Additionally, HPC generally features lower water-to-cementitious materials ratio (w/cm). Coupled with the inclusion of supplemental cementitious materials, HPCs promote dramatic improvements in concrete quality and durability. The use of HPC produces contemporary precast/prestressed concrete bridges that are both economical and possess long life expectancies. Accordingly, precast prestressed concrete bridges are vital to building and maintaining a sustainable transportation infrastructure supporting our economy and well-being of the United States.

Efficient design of prestress concrete bridges demands accurate prediction of prestress losses. The four major sources of prestress losses are elastic shortening (ES), creep (CR), shrinkage (SH) and relaxation (RE). Seating losses also occur but are usually not as significant as the other losses. Prestress losses are affected by structural detailing like the number and size of prestressing strands, the eccentricity of the prestressing force, girder spacing and girder spans. Additionally, prestress losses are affected by variations in material properties of the concrete. The concrete's Elastic Modulus, its Creep Coefficient and its shrinkage characteristics are all affected by the mix proportioning and by the overall quality of aggregates, the aggregates' shape and size, and mix proportioning. The variables in concrete material properties are largely unaccounted for in traditional computations for prestress losses, particularly when contract and construction processes decouple design functions from fabrication and construction. Numerous research programs have been conducted and a variety of prestress loss prediction methods have been proposed [NCHRP Report 496 by Tadros et al.<sup>13</sup>, Huo, Omasi and Tadros<sup>5</sup>]. However, the accurate determination of prestress losses has always challenged the prestressed concrete industry. Inaccurate predictions of losses often result in large cambers of prestressed concrete bridge girders, and by differential cambers in girders of identical design for the same spans on the same bridge. Excessive camber can, in turn, adversely affect the bridges' serviceability. Poor prediction of prestress losses can lead to increasing the number of prestressing strands, which can lead to increased cambers and increased incidence of cracking in end regions, adversely affecting durability, ride quality, and overall performance of the bridge.

The primary objective of this research is to (1) present various methods of computing prestress losses including older PCI methods and methods found in current AASHTO-LRFD, (2) investigate the inclusion of mild reinforcement and fully tensioned top strands, (3) develop a time-step methodology that accounts for recent changes to the AASHTO, and (4) to compare the results. Results show that both the inclusion of fully tensioned top strands and the inclusion of mild steel in the cross section produce effects that reduce prestress losses and also reduce excessive cambers. And while the results show the inclusion of fully tensioned top strand and non-prestressed mild

steel produce only small reductions on prestress losses, the inclusion of those items produce dramatic and large reductions in predicted cambers for bridge girders that should translate into improvements in bridge performance and ride quality.

## **BACKGROUND**

The ACI-ASCE Joint Committee 423 (1958) proposed the lump sum prestress loss estimates. These losses included the effects of creep, shrinkage and relaxation, but excluded the frictional and anchorage losses. The further refinement of losses led to the development of the PCI Committee recommendations (1975), the AASHTO-LRFD method (1977) and the ACI-ASCE Committee recommendations (1979). These methods for the calculation of losses failed to acknowledge the variability of material properties of concrete which then led to either overestimation or underestimation of losses [Shenoy and Frantz<sup>12</sup>, Gruel et al.,<sup>3</sup>, NCHRP Report 496<sup>13</sup>, Hale and Russell<sup>4</sup>]

The National Cooperative Highway Research Program [NCHRP Report 496<sup>13</sup>] investigated the measurement of material properties including elastic modulus, concrete strength, volume to surface ratio and creep coefficient and their effect on measured prestress losses and deflections. Further new equations for prestress losses were proposed. The experimental research programs performed on prestressed concrete bridge girders by Tadros et al.<sup>13</sup>, Gruel et al.<sup>3</sup>, Pessiki et al.<sup>10</sup> and Hale and Russell<sup>4</sup> verified that the PCI Design Handbook method and AASHTO-LRFD (1998) equations overestimated the prestress losses. However, the issues in camber and deflection were not discussed in detail, but it was concluded that accurate determination of losses was mandatory for the exact prediction of camber/deflection.

## **METHODOLOGY**

The analyses in this paper are based on an actual bridge that was built in or about the year 2000 on the John Kilpatrick Turnpike in Oklahoma as the North Canadian River Overflow Structure. This bridge features nineteen spans in both northbound and southbound directions with Type IV girders spanning 103 ft- 4 in. (31.8 m) (c/c bearing). The cast-in-place deck slab is 8 in. (203.2 mm) thick and consists of concrete with  $f'_c = 5000$  psi (34.5 MPa). Both northbound and southbound structures are 41 ft. (12.5 m) wide with five girders spaced at 8 ft.- 9 in. (2.7 m) Only the designs for interior girders are considered for this paper.



**Figure 1. North Canadian River Overflow Structure, John Kilpatrick Turnpike, Oklahoma, consistently of nineteen 103'-4" spans in both northbound and southbound directions with Type IV Girders spaced at 8'-0 centers.**



**Figure 2. View underneath the North Canadian Overflow Structure. John Kilpatrick Turnpike, Oklahoma.**

Photographs of the Overflow Structure are shown in Figure 1 and Figure 2. Figure 3 shows the cross section of the Type IV girder with strand patterns at mid-span. Two Top Strands are shown in the figure for illustration, but the number of top strands (0, 2 or 4) was a variable in this research. The original design and actual construction was

done with six draped strands. For our research, strand patterns were converted to straight strand patterns following current practice in Oklahoma. Debonding was provided at end regions to control compressive stresses at release.

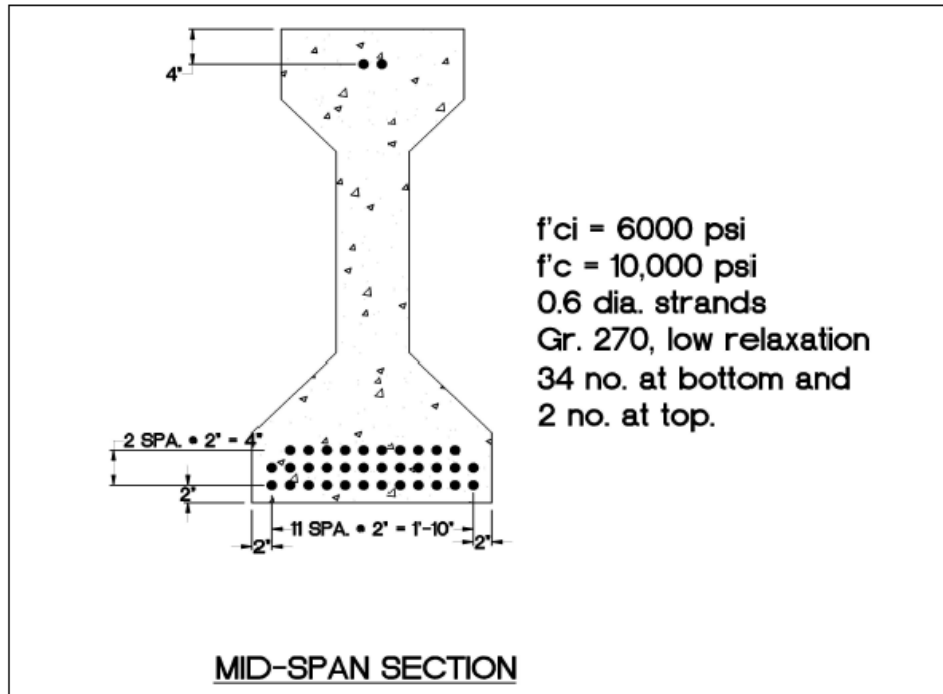


**Figure 3. Type IV Cross Section with thirty-four (34) 0.6 in strands in the bottom flange.**

In the analyses performed for this paper, Prestress Losses were computed at both the end spans and at mid-span. Methods to compute or estimate prestress losses are listed below.

- 1) PCI Handbook Method based on Zia et al (1979).
- 2) PCI Handbook Method but using transformed cross section properties in lieu of gross properties.
- 3) AASHTO LRFD Bridge Design Specifications (2014), Approximate Estimates of Total Losses
- 4) AASHTO LRFD Bridge Design Specifications (2014). Refined Estimates of Time-Dependent Losses
- 5) The Jayaseelan Time Step Method developed by the authors, adopting time-dependent formulations from ACI 209, AASHTO (2014), and other relevant sources.

The primary purpose of this paper is to investigate variations in prestress losses and in bridge girder camber that result from the following variables:

- a) Differences in Methodology;
- b) Inclusion of Fully-Tensioned Top Strand (none, 2 or 4 strands);
- c) Inclusion of non-prestressed mild reinforcement (none, 2.4 in<sup>2</sup> or 5.0 in<sup>2</sup>) (zero, 1548 mm<sup>2</sup> or 3226 mm<sup>2</sup>) at the CGS of the prestressing strand.

## METHODS AND RESULTS

All of the various methods described were used to produce results for “Base Case,” for T2 and T4 cases, and for MS 2.4 and MS 5.0 cases. The “Base Case” represents the design without top strand and without mild steel. The T2 and T4 cases are computed for designs where there are either two (T2) or four (T4) fully tensioned top strands. The MS 2.4 case includes four (4) #7 mild reinforcing bars at the center of gravity of the prestressing strands and the MS 4.0 case includes five (5) #9 mild reinforcing bars at the center of gravity of the prestressing strands. All cases and all methods employed a spreadsheet algorithm to compute prestress losses.

### PCI Handbook Method (Zia et al, 1979)

The PCI Handbook Method when published, represented the best descriptive method quantifying factors that influenced prestress losses. Even though the years have brought more detailed and perhaps more precise methods of estimating losses, the original paper remains a valuable tool for estimating prestressed losses for all types of precast/prestressed concrete structural members. And while the method may now be used primarily with building products, the principles set forth in its simple methodology are time tested and remain valid.

In our analysis, gross section properties were used. All of the stress parameters,  $f_{cpb}$ ,  $f_{cir}$ ,  $f_g$ ,  $f_{cds}$ , etc. are computed as described in the paper.  $K_{es}$  is taken as 1.0 for pre-tensioned concrete and  $K_{cir}$  is used as 0.90 without alteration or iteration.  $K_{cr}$  is 2.0 and  $K_{sh}$  is 1.0 for pretensioned members.  $P_{pi}$  is computed from  $A_{ps} * 0.75 f_{pu}$  and seating losses occur at tensioning before other losses occur. The elastic modulus of strand,  $E_{ps}$  is taken as 28,500 ksi (196.5 GPa) and the elastic modulus of concrete, whether  $E_{ci}$  or  $E_c$  was estimated using ACI 318-14 equation (ACI 310-14 Section 19.2.2.1.a)<sup>2</sup>.

$$E_c = 33w^{1.5} \left( f'_c \right)^{0.5}$$

Computed losses from the PCI Handbook Method are reported in **Table 1**. Note that the method can account for the effects of Top Strand as the total prestress force  $P_{pi}$  and its eccentricity,  $e$ , change with changes in strand patterns. On the other hand, the method does not have a mechanism to account for the effects of mild steel. Shrinkage Loss ( $SH$ ) is the same for all cases, as  $SH$  is dependent upon the assumed ultimate shrinkage strain ( $550 \times 10^{-6}$  in/in), the relative humidity ( $RH$ , 65% for Central Oklahoma) and the  $V/S$  ratio which do not change from case to case.  $CR$  is computed in the same method for either 90 days or 10 years, and different values for  $CR$  are reported for the two time steps. But the method doesn't truly account for the effects of time; instead the difference in computation comes solely from the differences in concrete stress resulting from sustained dead load. At 90 days, the slab's dead load is not included in  $f_{cds}$  and at 10 years the dead load from the slab is included. We note that the “base case” (no top strand, no mild steel) shows a prestress loss of 53.5 ksi (368.9 MPa) and that the inclusion of Top Strand (T4) is shown to reduce the TL to 48.5 ksi (334.4 MPa). Using the PCI Handbook method, the inclusion of top strand is shown to reduce TL from 53.5 to 48.5 ksi.

### **PCI Handbook Method using Transformed Cross Section Properties**

Prestress losses were computed using Transformed Cross Section Properties. In this analysis, all of the stress parameters for the PCI Handbook Method are computed using transformed cross sections. One of the differences when using transformed properties is that a value for  $f_{cpi}$  is not needed for  $ES$  computations; instead  $f_{cir}$  is computed directly using transformed properties with  $K_{cir}$  is taken as 1.0.  $ES$  becomes a more direct computation once transformed properties are computed. Other parameters are computed in the same manner and same formulae but using transformed section properties in place of gross section properties. Note that when using transformed section properties, the inclusion of mild steel affects the computations for losses, and in this manner the effects of mild steel can be included.

Like the PCI Method (using gross section properties),  $SH$  is the same for all cases since the inclusion of additional reinforcement does not affect the  $RH$  nor the  $V/S$  ratio.  $CR$  reflects minor changes created by inclusion of the Top Strand and Mild Steel. The small changes in  $CR$  reflect the effects of the top steel, its effects on prestressed eccentricity, and its inclusion in the transformed cross section properties. **Table 2** reports losses computed using this method.

### **AASHTO-LRFD Approximate Estimates of Time Dependent Losses.**

Computation of losses for this analysis follows the methods and procedures taken from the AASHTO-LRFD Bridge Design Specifications, 7<sup>th</sup>, 2014. Estimates of for long term losses resulting from creep and shrinkage of concrete, and for relaxation of steel ( $CR+SH+ES$ ) were calculated using AASHTO LRFD (2014) Eq. 5.9.5.3-1b<sup>7</sup>. Elastic shortening ( $ES$ ) is computed independently in the prescribed method (which closely resembles other methods). Total Loss ( $TL$ ) is obtained by adding  $ES$  to the estimate for time-dependent losses ( $CR+SH+RE$ ). Results for prestress losses computed in the method are found in **Table 3**. The equations do not account for the inclusion of mild steel. The addition of fully tensioned top strands affects both  $ES$  and also changes the parameters in the equation for long term losses. So changes due to fully top strands are reflected in the **Table 3** even though the changes are relatively small.

### **AASHTO-LRFD Refined Estimate of Losses**

Computation of losses for this analysis follows the methods and procedures taken from the AASHTO-LRFD Bridge Design Specifications, 7<sup>th</sup>, 2014. Article (5.9.5.4.1)<sup>7</sup>. Prestress losses were calculated at mid-span in two stages as specified in the code, losses at time of transfer and time of deck placement and time of deck placement to final time. The shrinkage gain due to shrinkage of deck of concrete was not considered in this research paper. Results from the Refined Estimates of Time Dependent Losses are reported in **Table 4**. The method produces surprisingly stable creep losses ( $CR$ ) from slab casting through the life of the structure. Also, the Refined Method does not account for the effects of mild steel that could be included in the cross section.

### Jayaseelan Time Step Method

In this method time was divided into intervals where the duration of each time interval was made larger as the age of concrete increases. The prestress losses and the stresses in the concrete at the end of each interval were calculated. The calculated stresses include the elastic stresses due to prestress, gravity loads and sustained loads along with the time dependent effects due to creep and shrinkage of concrete. After slab casting, the whole composite section of concrete is treated as an elastic material. The elastic stresses and the stresses due to creep strain in concrete were individually calculated. This method takes into account the varying material properties by re-computing the concrete properties each day. The initial time on the transfer of prestress was at  $t_i = 1$  day, slab was cast at  $t = 90$  days and superimposed loads were applied at  $t = 120$  days respectively. The final prestress losses were calculated at  $t = 10$  years.

### Time Dependent equations

The Time Step method calculated the concrete strength ( $f'c$ ) using the ACI 209R eq2-1<sup>1</sup> as specified below:

$$(f'c)_t = \frac{t}{\alpha + \beta t} (f'c)_{28}$$

where:

$\alpha$  and  $\beta$  = constants

$t$  = age of the concrete in days

$(f'c)_{28}$  = specified 28 day compressive strength of concrete.

Time Dependent Creep and Shrinkage coefficients:

The Jayaseelan Time Step method used the following AASHTO LRFD (2014) time dependent equations for creep coefficient and shrinkage strain for the computation of prestress losses. The creep coefficient and shrinkage strain were calculated for every time interval as an increasing function of time. The initial time  $t_i$  was taken at 1 day.

### Creep Coefficient

$$\psi(t, t_i) = 1.9 k_s k_{hc} k_f k_{id} t_i^{-0.118} \quad (5.5.2.3.2-1)^7$$

in which:

$$k_s = 1.45 - 0.13(V/S) \geq 1.0 \quad (5.4.2.3.2-2)^7$$

$$k_{hc} = 1.56 - 0.008H \quad (5.4.2.3.2-3)^7$$

$$k_f = \frac{5}{1 + f'_{ci}} \quad (5.4.2.3.2-4)^7$$

$$k_{id} = \frac{t}{61 + 4f'_{ci} + t} \quad (5.4.2.3.2-5)^7$$

where:

$H$  = relative humidity.

$k_s$	=	factor for the effect of the volume-to-surface ratio of the component
$k_{hc}$	=	humidity factor for creep
$k_{td}$	=	time development factor
$t$	=	maturity of concrete
$t_i$	=	age of concrete at time of load application
$V/S$	=	volume-to-surface ratio

### ***Shrinkage Strain***

$$\varepsilon_{sh} = k_s k_{hs} k_f k_{td} 0.48 \times 10^{-3} \quad (5.4.2.3.3-1)^7$$

in which:

$$k_{hs} = (2.00 - 0.014H) \quad (5.4.2.3.3-2)^7$$

where:

$$k_{hs} = \text{humidity factor for shrinkage}$$

### ***Effective modulus or Reduced Modulus of Elasticity***

Gradual change in stress during the service life of a structure produces additional instantaneous and creep strains. These additional strains are superimposed on the creep strains due to initial stresses and to all previous stress changes. Due to concrete aging these additional strains are much less than those which would arise if the same stress changes occurred right after the instant of first loading. This effect is accounted for by the use of age adjusted effective modulus, originated by Trost (ACI 209R-92)<sup>1</sup>

In this paper the effective or the reduced modulus of elasticity combines the effect due to elastic strain and creep of concrete as an elastic deformation on concrete section. At a constant loading the elastic plus creep strain was calculated as  $[1 + \psi(t)]$  times the elastic strain. The effective modulus of elasticity for each day was calculated as follows:

$$E_{eff}(t) = \frac{E_c(t)}{\psi(t)}$$

where

$$\psi(t) = \text{creep coefficient at time } t$$

The effective modulus is reduced due to creep effects in the beam and the transformed cross section properties were further calculated based on this reduced effective modulus. The above equation was used for the time dependent analysis due to the effects of all the loads such as: initial prestress, self weight, deck weight and superimposed dead loads. The effective modular ratio  $n_{eff}$  is calculated using this reduced effective modulus  $E_{eff}$  as given below:



$$n_{eff} = \frac{E_{ps}}{E_{eff}}$$

where

$E_{ps}$  = modulus of elasticity of prestressing strands

$E_{eff}$  = effective modulus of elasticity of concrete

The effect due to time dependent creep was included by using the modular ratio  $n_{eff}$  in the calculation of transformed cross section properties.

Prestress Loss Equations

### ***Elastic Shortening***

The Elastic Shortening  $ES$  was calculated as given below:

$$ES = \frac{E_{ps}}{E_c} f_{cgp}$$

in which:

$$f_{cgp} = \left[ P_{pi} - A_{ps} (SH + RE) \right] * \left[ \frac{1}{A_{tr}} + \frac{e_{tr}^2}{I_{tr}} \right] - \left[ \frac{M_{S.W} * e_{tr}}{I_{tr}} \right]$$

where:

$f_{cgp}$  = the concrete stress at the center of gravity of prestressing tendons due to the prestressing force immediately after transfer and the self weight of the member at the section of maximum moment

$E_{ps}$  = modulus of Elasticity of prestressing steel

$E_{ct}$  = modulus of Elasticity of concrete at transfer or time of load application

$P_{pi}$  = initial prestressing force in the prestressing strands

$A_{ps}$  = area of prestressing strands

$A_{tr}$  = transformed cross- sectional area

$e_{tr}$  = eccentricity of the prestressing strands calculated using transformed cross section properties

$I_{tr}$  = transformed moment of inertia of the section

$M_{S.W}$  = moment due to self weight of the girder

The first term in the square brackets accounts for the reduction in prestressing force due to the effects of shrinkage of concrete and relaxation in prestressing steel. The calculation of  $f_{cgp}$  for the loading stage after slab casting, utilizes the composite transformed cross section properties of concrete calculated with the use of effective modulus.

### **Creep loss**

Incremental creep strains were computed on a day to day basis using the formula:

$$\Delta \varepsilon_{cr}(t) = \frac{1}{E_c(t)} f_{cgp} [\psi(t,1) - \psi(t-1,1)]$$

where

$\Delta \varepsilon_{cr}(t)$  = incremental creep strain at time  $t$

$\psi(t, t_i)$  = creep coefficient calculated using AASHTO LRFD (2014) Eq. (5.4.2.3.2-1)<sup>7</sup>

The creep loss was calculated as given below:

$$CR(t) = CR(t-1) + \Delta \varepsilon_{cr}(t) * E_{ps}$$

The calculated final creep loss was calibrated to yield the same results as the creep loss calculated using AASHTO LRFD refined method.

### **Shrinkage Loss**

The shrinkage of concrete depends on the volume to surface ratio and relative humidity, but is independent of the loading and is caused primarily due to shrinkage of cement paste. Following equation was used to calculate the shrinkage loss for everyday.

$$SH(t) = E_{ps} * \varepsilon_{sh}(t) * K_{sh}$$

in which,

$$K_{sh} = \frac{\left( \frac{1}{A_{tr}} + \frac{e_{tr}^2}{I_{tr}} \right)}{\left( \frac{1}{A_g} + \frac{e_g^2}{I_g} \right)}$$

where:

$\varepsilon_{sh}(t)$  = shrinkage strain at time  $t$  calculated using AASHTO LRFD (2014) Eq. (5.4.2.3.3-1)<sup>7</sup>

$K_{sh}$  = transformed cross section coefficient that accounts for the time-dependent interaction between concrete and prestressing steel.

$A_g$  = gross cross-sectional area

$e_g$  = eccentricity of the prestressing strands calculated using gross cross section properties

$I_g$  = gross moment of inertia of the section

### **Relaxation Loss**

Gr. 270 Low relaxation strands are most widely used in prestressed girders. The time dependent relaxation loss is calculated using the proposed formula in NCHRP Report 496<sup>13</sup>

$$RE(t) = \left[ \frac{f_{pt}}{K'_L} \frac{\log(24t + 1)}{\log(24t_i + 1)} \left( \frac{f_{pt}}{f_{py}} - 0.55 \right) \right] \left[ 1 - \frac{3(SH(t) + CR(t))}{f_{pt}} \right]$$

where:

$f_{pt}$  = initial prestress in prestressing strands immediately after transfer

$f_{py}$  = specified yield strength of prestressing steel

$K'_L$  = 45 for low relaxation strands

Total Loss for the Time Step method was calculated by summing up the losses for each day.

$$TL = ES + CR(t) + SH(t) + RE(t) \quad (12)$$

The resulting prestress,  $f_{se}$  and the corresponding prestress force  $F_{se}$  were calculated for each day and each stage of loading.

### Computation of Concrete stresses and strains:

The top fiber stress, ( $f_t$ ) and bottom fiber stresses ( $f_b$ ) due to both prestress and gravity were calculated for each day. The corresponding strains ( $C_t = f_t/E_{eff}$ ,  $C_b = f_b/E_{eff}$ ) were also calculated for the respective stresses. All calculations used the transformed cross section properties of the girder section. The composite transformed cross section properties of concrete were calculated after 90 days of slab cast. After slab cast the additional strain due to creep was calculated by applying a resultant force on the composite cross section of the beam. This resultant force was calculated from the change in stress at time ( $t$ ) due to creep in the beam. The final concrete strains at  $t = 10,000$  days includes: the strain due to the prestressing force, gravity loads, slab wt, super imposed dead loads and the additional strain due to time dependent creep effects. Prestress losses and top and bottom stresses were computed on a day to day basis for both ends and mid-span of the section. The results for prestress losses computed using the Jayaseelan Time Step method is reported in **Table 5**. From Figure 4 we can see that the final prestress losses calculated using Jayaseelan time Step method are comparable to the losses computed using the PCI and the AASHTO LRFD methods.

### Computation of Girder Cambers

Experience has proved that it is difficult to accurately predict cambers in prestressed concrete beams. This principally due to the variation of the modulus of elasticity of concrete, creep of concrete, age of concrete, actual support conditions, temperature and shrinkage differential between top and bottom fibers, and variation in properties between top and bottom of concrete [Lin and Burns]<sup>6</sup>.

In Jayaseelan time step method, the camber of the beam due to prestress at both mid-span and end-span; deflection of the beam due to gravity and live loads at mid-span were directly computed from the curvature due to concrete strains using moment area method. The camber and deflections were calculated for everyday. The variations in material properties due to the change in the age of concrete, modulus of elasticity and creep of concrete has been

taken into consideration. After slab cast the camber due to the additional creep strain was also included in the final deflection. **Table 6** reports the camber calculations at 1 day, 90, 91 and long-term deflections at 10,000 days.

**Figures 7, 8 and 9** show the variation of camber with time for various cases. We can see that there is a significant reduction in camber at 91 days, due to the dead weight of the slab and also a reduction of camber at 120 days due to super imposed dead loads.

## RESULTS AND DISCUSSION – PRESTRESS LOSSES

### The Five Methods

Results from the five different methodologies are presented in Tables 1 through 5. The tables all report the prestress losses at midspan. Losses at the girder ends were computed but not reported. The methods include the PCI Handbook Method based on the paper by Zia et al (1979), the PCI Handbook Method Method but modified by using transformed section properties, both the AASHTO-LRFD 2014 Approximate Method and the Refined Method, and the Jayaseelan Time Step Method developed by the authors. The tables provide details of the various components of prestress losses where possible, *ES*, *CR*, *SH* and *RE*.

**Table 1. Prestress Losses at mid-span calculated using Gross-Section Properties with PCI Design Hand Book Method**

Case	Concrete Age	ES	CR	SH	RE	Losses at mid-span
		(ksi)	(ksi)	(ksi)	(ksi)	(ksi)
Base	90 days	17.5	27.2	5.8	3.0	53.5
	10 years	17.5	13.3	5.8	3.5	40.1
T2	90 days	16.3	25.3	5.8	3.1	50.5
	10 years	16.3	13.0	5.8	3.6	38.7
T4	90 days	15.5	24.0	5.8	3.2	48.5
	10 years	15.5	13.2	5.8	3.6	38.1
MS.2.4	90 days	<b>Prestress Losses Same as Base Case</b>				
	10 years					
MS 5.0	90 days					
	10 years					

**Table 2. Prestress Losses at mid-span calculated using Transformed Cross-Section Properties with PCI Design Hand Book Method**

Case	Concrete Age	ES	CR	SH	RE	Losses at mid-span
		(ksi)	(ksi)	(ksi)	(ksi)	(ksi)
Base	90 days	18.2	28.2	5.8	2.9	55.1
	10 years	18.2	15.6	5.8	3.4	43.0
T2	90 days	17.0	26.4	5.8	3.0	52.2
	10 years	17.0	15.2	5.8	3.5	41.5
T4	90 days	16.3	25.2	5.8	3.1	50.3
	10 years	16.3	15.3	5.8	3.5	40.8
MS.2.4	90 days	17.6	27.2	5.8	3.0	53.5
	10 years	17.6	15.1	5.8	3.5	41.9
MS 5.0	90 days	17.0	26.3	5.8	3.0	52.1
	10 years	17.0	14.6	5.8	3.5	40.8

**Table 3. AASHTO LRFD Bridge Design Specifications (2014), Approximate Estimates of Total Losses**

Case	ES	CR+SH+RE	Losses at mid-span
	(ksi)	(ksi)	(ksi)
Base	20.2	25.6	45.8
T2	18.8	26.4	45.2
T4	17.8	27.3	45.1
MS 2.4	Prestress Losses Same as Base Case		
MS 5.0			

**Table 4. AASHTO LRFD Bridge Design Specifications (2014), Refined Estimates of Time-Dependent Losses at mid-span calculated using Gross Section properties**

Case	Concrete Age	ES	CR	SH	RE	Losses at mid-span
		(ksi)	(ksi)	(ksi)	(ksi)	(ksi)
Base	90 days	20.2	14.1	5.1	1.2	40.6
	10 years	20.2	13.3	7.1	2.4	43.1
T2	90 days	18.8	13.3	5.2	1.3	38.4
	10 years	18.8	12.5	7.2	2.5	41.0
T4	90 days	17.8	12.7	5.2	1.3	37.0
	10 years	17.8	12.0	7.2	2.6	39.6
MS.2.4	90 days	Prestress Losses Same as Base Case				
	10 years					
MS 5.0	90 days					
	10 years					

**Table 5. Jayaseelan Time Step Method, Prestress losses at mid-span**

Case	Concrete Age	ES	CR	SH	RE	Losses at mid-span
		(ksi)	(ksi)	(ksi)	(ksi)	(ksi)
Base	90 days	18.3	14.8	5.6	1.1	39.8
	10 years	18.3	13.3	7.8	2.2	41.6
T2	90 days	17.1	13.9	5.7	1.2	37.8
	10 years	17.1	12.2	7.8	2.4	39.5
T4	90 days	16.3	13.3	5.7	1.2	36.5
	10 years	16.3	11.5	7.9	2.4	38.2
MS.2.4	90 days	17.7	14.1	5.4	1.1	38.3
	10 years	17.7	12.6	7.5	2.3	40.1
MS 5.0	90 days	17.0	13.4	5.2	1.2	36.9
	10 years	17.0	12.0	7.2	2.4	38.7

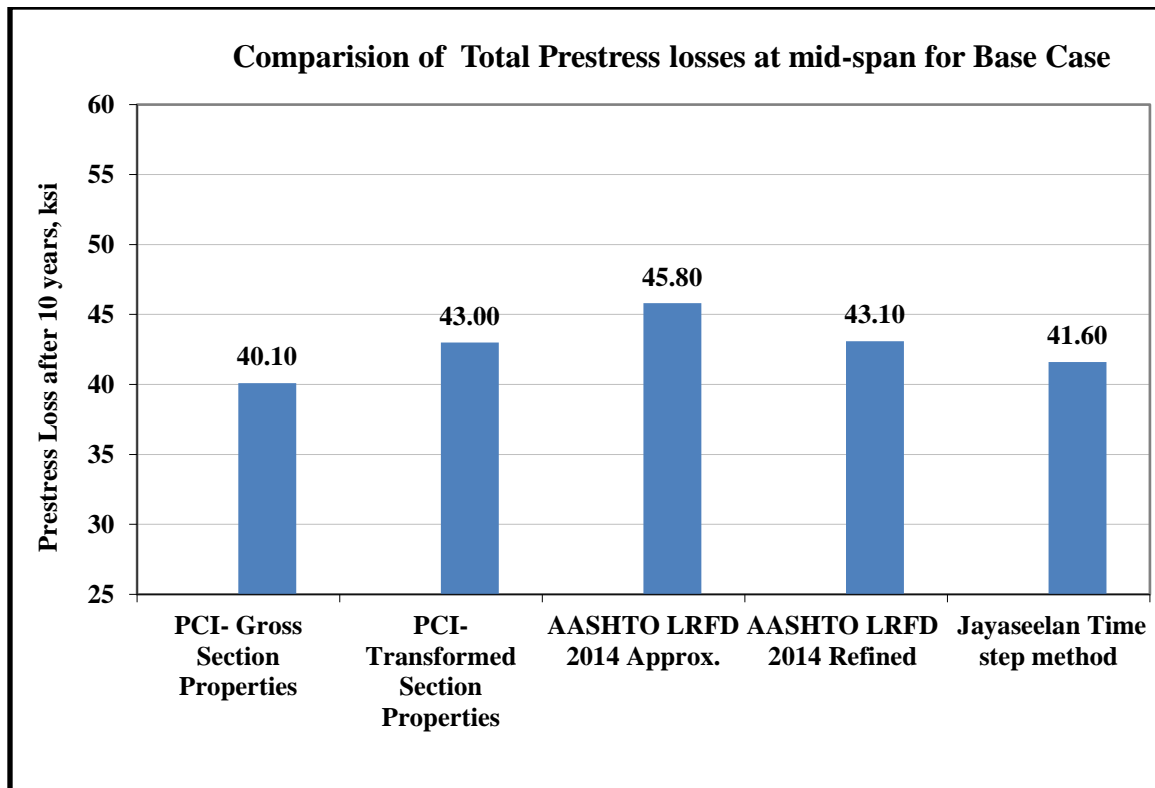


Figure 4. Comparison of Total Prestress Losses at mid-span for Base Case. Note: 1 ksi = 6895 kPa.

When looking at the Total Losses ( $TL$ ) for each method, the results are probably most remarkable for the similarities in  $TL$  that is found. For the “Base Case” design, the  $TL$  for each of the five methods falls between 40.10 ksi (276.5 MPa) and 45.80 ksi (276 and 316 MPa), or between 19.8% and 22.6% of total prestressing force. The results for Total Loss ( $TL$ ) using the “Base Case” design and the five different methods are pictured in **Figure 4**. **Figure 4** captures the relative uniformity between the different methods. The takeaway from this analysis is that, at least for the “Base Case” design, the  $TL$  estimated using any one of the five methods produces a result that is very near to one another. In order to view the relative importance of the magnitude of the differences, consider the impact on the number of prestressing strands required to fulfill the design requirements. If the “Base Case” contains 34 bottom strands, a 2 percent difference in the Total Loss ( $TL$ ) is only about 0.7 strands. This number means that two strand difference may occur in about one-third of similar design cases when using one of these five methods. This result is small enough to encourage a designer of precast prestressed bridge girders to use an approximate method for estimating prestress losses as a more precise analysis may only change one in three strand designs.

#### Effects of Fully Bonded Top Strands

With regard to the *Inclusion of Fully Tensioned Top Strands*, there is a clear trend that the Top Strands reduce overall prestress losses. For the PCI Handbook Method, the “T2” case reduces  $TL$  from 40.1 to 38.7 ksi (276 to 267

MPa) and the “T4” design further reduces *TL* to 38.1 ksi (263 MPa). For the AASHTO 2014 Refined Losses method, the Inclusion of Top Strands reduces the “Base Case” from 43.1 to 41.0 ksi (297 to 283 MPa) with “T2” and 39.6 ksi (273 MPa) with “T4.” So in a very real way, the use of four fully tensioned top strands (T4) has the effect of reducing prestress losses from 21.3% of total prestress to about 19.6%. The conclusion from this analysis would be that the Inclusion of Top Strand has a small but certain effect on reducing the *TL*.

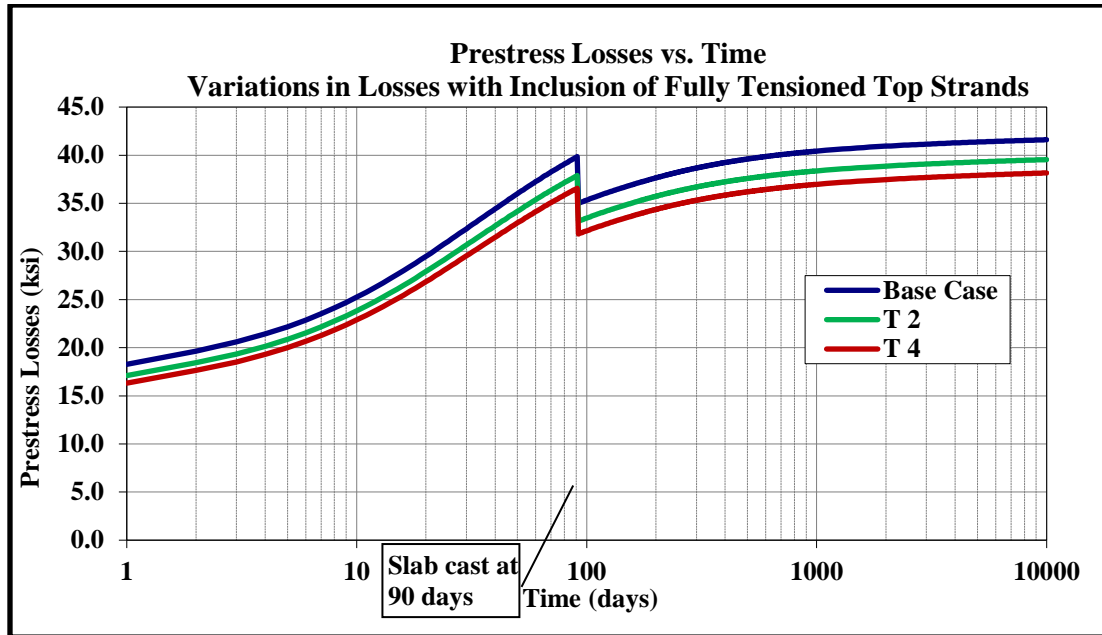


**Figure 5. Prestress Losses vs. Time at mid-span using the Jayaseelan Time Step method. Variations in losses are charted to show variations resulting for Inclusion of Full-Tensioned Top Strands. Note: 1 ksi = 6895kPa.**

This result is further supported by the Figure 5 which charts the prestress losses over time. **Figure 5** plots the prestress losses using the Jayaseelan Time Step formulations. *TL* is plotted for a log scale of time expressed in days. One can see from the figure that the inclusion of Top Strands has the effect of reducing *TL* from that of the Base Case, and that this effect is carried through the life of the structure.

### Effects of Mild Steel

Based on engineering mechanics, it is known that the inclusion of mild steel reduces prestress losses when included in prestressed concrete. As concrete shortens whether through elastic shortening, creep or shrinkage, the shortening causes additional compressive strains and stresses in the composite anchored mild steel, thus redistributing the forces within a prestressed concrete cross section that actively resist the prestressing forces. In a very real way, the mild steel provides an ever enlarging “transformed” cross section that reduces the time-dependent shortening in concrete and thereby reduces the total losses.

Despite this, the calculations for three of the five methods for computing losses are unaffected by the inclusion of mild steel. These three methods, the PCI Handbook Method (using gross section properties), the AASHTO



Approximate Method and the AASHTO Refined Method do not contain mechanisms within their procedures that account for the inclusion of mild steel. So, if one uses these methods then the inclusion of mild steel has no effect on the *TL* estimate.

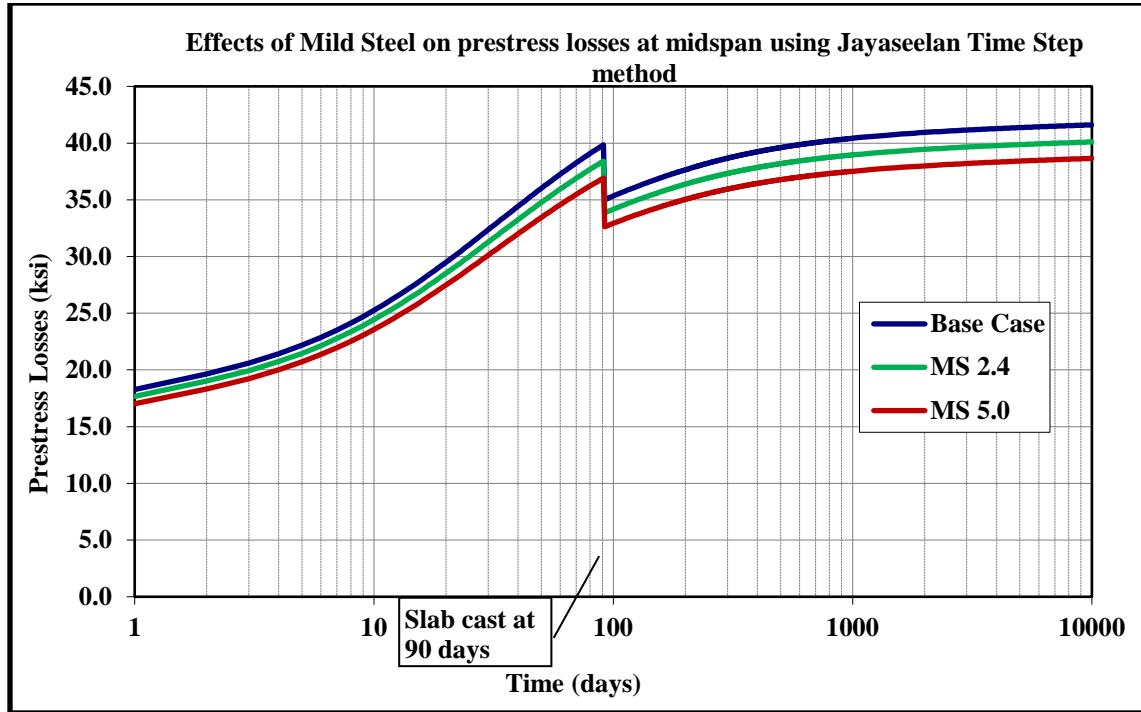


**Figure 6. Effects of Mild Steel on Prestress Losses at mid-span using Jayaseelan Time Step method. Note: 1 ksi = 6895 kPa.**

The two remaining methods both incorporate the effects of mild steel, the PCI Method (using transformed properties) and the Jayaseelan Time Step method. The analysis shows a clear trend where the inclusion of mild steel has the effect of reducing prestress losses. For the PCI Handbook Method using transformed properties, the “MS 2.4” case reduces *TL* from 43.0 to 41.9 ksi (296 to 289 MPa) and the “MS 5.0” design further reduces TL to 40.8 ksi (279 MPa). For the Jayaseelan Time Step method, the Inclusion of Mild Steel reduces the “Base Case” from 41.6 to 40.1 ksi (296 to 276 Mpa) with “MS 2.4” and 38.7 ksi (267 MPa) with “MS 5.0.” So, the use of five #9 bars (MS 5.0) has the effect of reducing prestress losses from 20.5% of total prestress to about 19.1%. The conclusion from this analysis would be that the Inclusion of Mild Steel produces small but certain effects on overall prestress losses.

This result is illustrated in Figure 6 which charts the prestress losses over time with values computed using the Jayaseelan Time Step formulations. The figure clearly shows that the inclusion of Mild Steel has the overall effect of reducing prestress losses. Furthermore, these reductions in *TL* are carried through over the life of the structure. Even so, the effects of including Mild Steel only account for saving about 2% of total prestress.

## RESULTS AND DISCUSSION – BRIDGE GIRDER CAMBER

The section above demonstrates that both the Inclusion of Top Strand and the Inclusion of Mild Steel produce mildly positive effects in reducing the total amount of prestress loss (*TL*). From that, a designer or bridge owner may not be overwhelmingly convinced to incorporate either technique into their designs based solely on the evidence from Prestress Losses. However, as this section will demonstrate, the effects of both Top Strands and Mild Steel are much more profound in influencing the Camber (or deflections) of Bridge Girders and the bridges they are made part of. It is through these arguments where some designers and some bridge owners might be convinced that incorporating these devices will help with ease of construction and help with long term serviceability of their precast prestressed concrete bridges.

**Table 6. Jayaseelan Time Step method, Camber Estimation at mid-span**

Case	Camber at 1 day after release	Camber at 90 days, prior to slab cast	Camber at 91 days after slab cast	Long Term Camber at mid-span
	(in)	(in)	(in)	(in)
<b>Base</b>	-2.98	-4.08	-2.17	<b>-1.81</b>
<b>T2</b>	-2.73	-3.77	-1.81	<b>-1.42</b>
<b>T4</b>	-2.48	-3.44	-1.43	<b>-1.00</b>
<b>MS 2.4</b>	-2.88	-3.84	-1.98	<b>-1.59</b>
<b>MS 5.0</b>	-2.77	-3.58	-1.78	<b>-1.37</b>

In NCHRP 496 Report<sup>13</sup>, their primary recommendation for future research was to investigate Camber in Bridges. This part of our paper responds to that need, and shows purpose for the additional of Top Strands and Mild Steel to standard bridge girder design. In this paper, the computations for stress and strain are embedded in our methodology. **Table 5** reports losses at midspan, and within those calculations we can also compute the curvature of the cross section at midspan. To provide accurate estimates for girder camber, the prestress losses and material stresses were also required at the end of the spans. Additionally, the dead load deflections were also computed. Altogether, the camber calculations reported in **Table 6** and in the figures that follow account for varying prestress forces along the length of the bridge span and also incorporate the downward deflections due to self-weight of the girder, and all other superimposed dead loads.

Within **Table 6**, cambers are reported at 1 day (immediately after release), at 90 days (prior to slab casting), at 91 days (after slab casting) and at 10,000 days, which is taken as approximately equivalent to the life span of the bridge. Immediately after release, the camber for the “Base Case” is nearly 2.98 in. (76 mm). Through the effects of creep over the next 90 days, the camber increases more than an inch to 4.08 in. (104 mm) prior to slab casting.

Not accounted for in our analysis is the probability that support conditions during handling, storage and transport vary and also contribute to camber of the pretensioned beam. **Table 6** also reports the camber is 2.17 in. (55 mm) after slab casting (for the “Base Case”). This means simply that more than two inches (50 mm) of haunch would be added to the beam depth at the ends of the beams during slab casting so that roadway elevations would be “flat.” During slab casting, the deflection resulting from the self-weight of the slab is 1.91 in. (49 mm). The long-term camber at 10,000 days includes the effects of super-imposed dead loads, principally the loads from diaphragms and parapets which in our models are applied at 120 days.

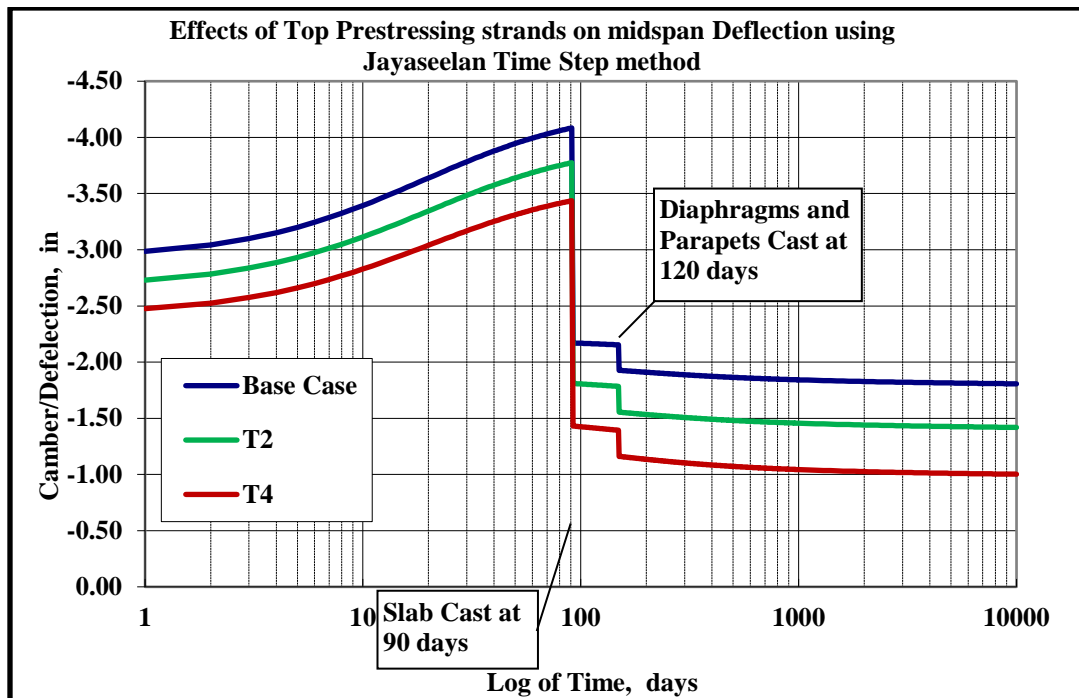


**Figure 7. Effects of Top Prestressing Strands on mid-span deflection using Jayaseelan Time Step method. Note: 1 in. = 25.4 mm.**

The effects of Fully Tensioned Top Strands are shown in Figure 7. From Figure 7 and **Table 6**, the inclusion of four top strands reduces initial camber (at one day) by about 0.50 in (12.7 mm). Figure 7 illustrates that as time increases, the differences in camber also increase, and at 90 days, the camber in the base case is 4.08 in. (104 mm) whereas the camber in the T4 design is 3.44 in. (87 mm), a reduction of 0.64 in. (16 mm). As time moves forward, the differential that results from including top strand also increases so that the long term decrease in camber is 0.81 in. (21 mm) out of a computed base case total of 1.81 in. (46 mm), representing a 45% decrease in the camber of the bridge.

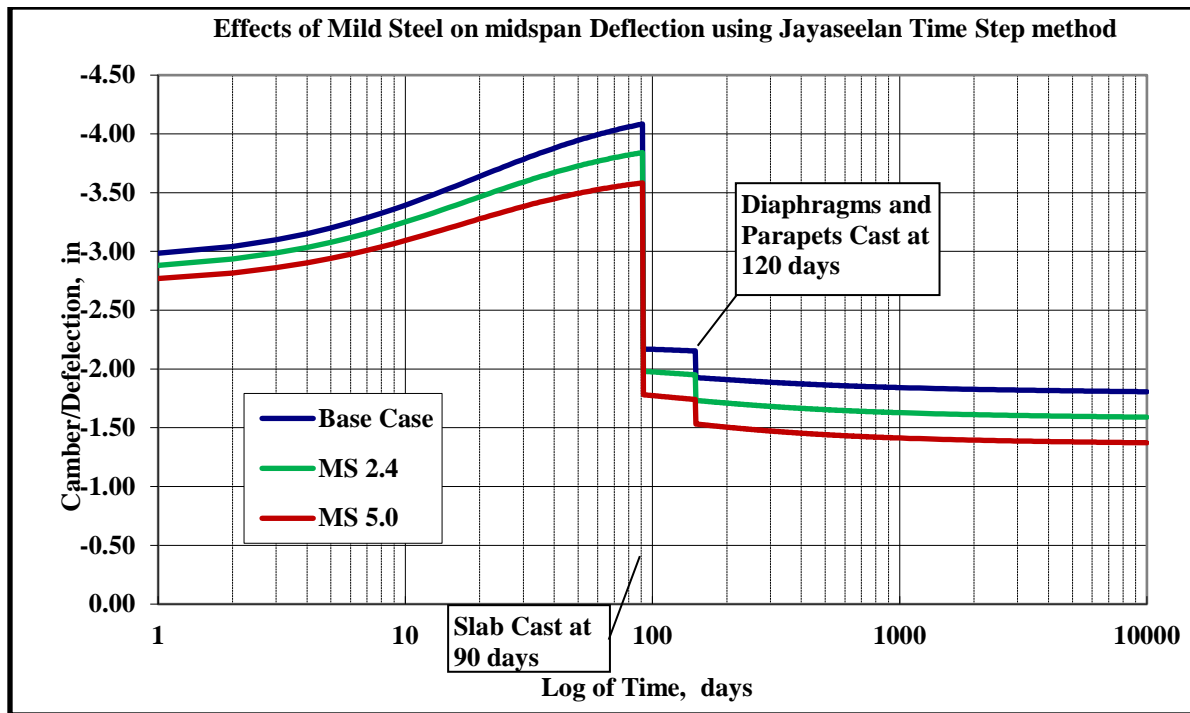


**Figure 8. Effects of Non-prestressing steel/Mild steel on mid-span deflection using Jayaseelan Time Step method Note: 1 in. = 25.4 mm.**

The effects of Including Mild Steel are shown in Figure 8. From Figure 8 and **Table 6**, the inclusion of five (5) #9 bars (MS 5.0) reduces initial camber (at one day) by about 0.20 in. (5 mm) Figure 8 illustrates that as time increases, the differences in camber also increase, and at 90 days, the camber in the base case is 4.08 in. (104 mm) and the camber in the MS 5.0 design is 3.58 in. (91 mm), a reduction of 0.50 in. (13 mm). As time moves forward, the differences in camber resulting the inclusion of Mild Steel also increases. The long term decrease in camber is significant. As **Table 6** reports, the long-term of the “Base Case” is 1.81 in. (46 mm) whereas the MS 5.0 design results in long-term camber of only 1.37 in. (35 mm), a 0.44 in. (11 mm) reduction representing about 25% of the camber from the “base case.”

Figure 9 shows the effect on Beam Camber when Fully Tensioned Top Strands are included with Mild Steel in the bottom flange. One can see from the figure that initial cambers, immediately after release are reduced from 2.98 in. (76 mm) to approximately 2.25 in. (57 mm), a reduction in initial cambers of about 0.75 in. (19 mm). At 90 days, the camber is reduced from 4.08 in. (104 mm) to less 3.0 in. (76 mm), a reduction in camber of more than 1.0 in. (25 mm). And long-term, Figure 9 shows that the reduction in Camber is approaching 1.5 in. (38 mm) by including Top Strand plus Mild Steel. For the design under investigation, an AASHTO Type IV bridge beam with composite deck slab spanning over 103 ft. (31 m) , the camber at slab construction is reduced by more than 1.0 in. (25 mm) to less than 3.0 in. (76 mm) and the long-term camber is reduced to 0.50 in. (13 mm) which means that the long-term position of the Type IV girder is nearly flat.

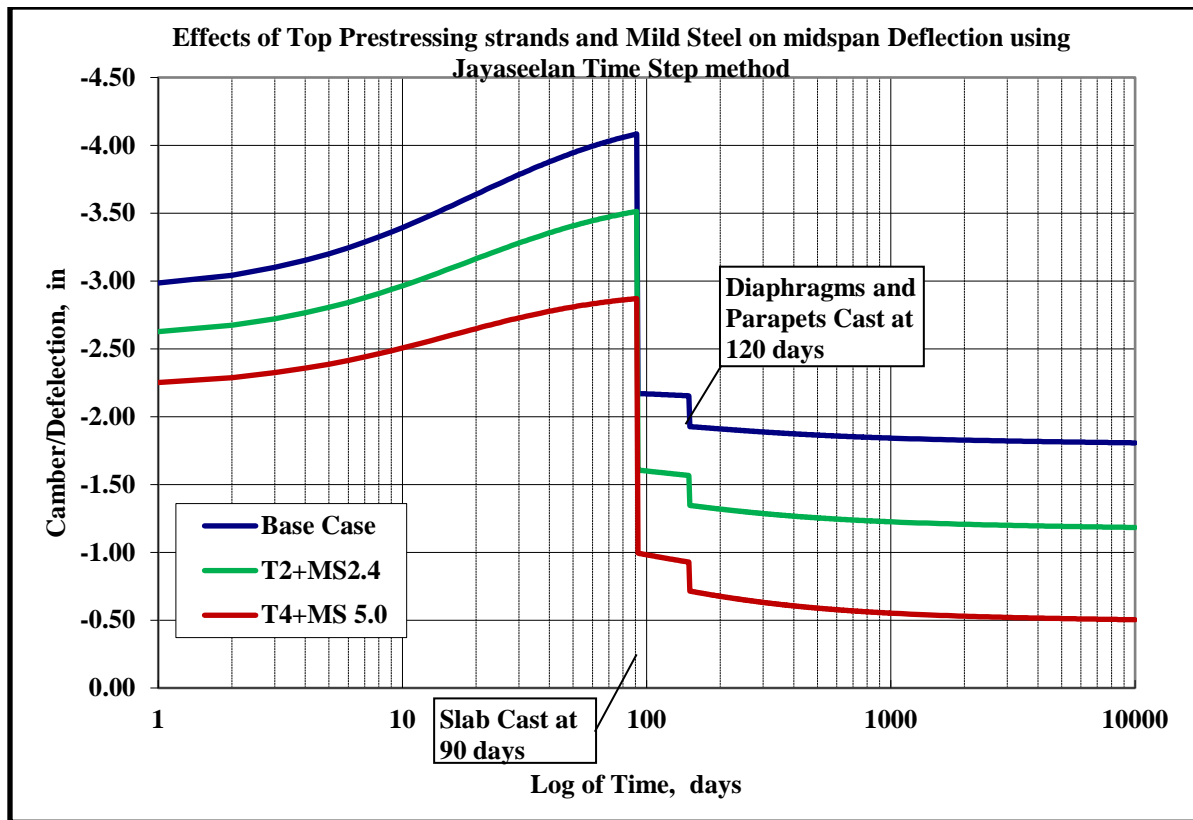


Figure 9. Effects of Top prestressing strands and Mild Steel on mid-span deflection using Jayaseelan Time Step method. Note: 1 in. = 25.4 mm.

## CONCLUSIONS AND RECOMMENDATIONS

1. For the design case examined, five different methods, developed from widely different approaches produced estimates for prestress losses that are very near to one another in result. For the “Base Case”, the PCI Handbook Method (Zia et al) produced a TL estimate of 40.1 ksi (276 MPa), 19.8% of total prestressing) whereas the AASHTO Refined Method produce a TL estimate of 43.1 ksi (297 MPa, 21.2%). The Jayaseelan Time Step Method produced a TL estimate of 41.6 ksi (287 MPa, 20.5%).
2. Neither the AASHTO Approximate method nor the AASHTO Refined method account for the inclusion of Mild Reinforcement and its effects on prestress losses.
3. The inclusion of Fully Tensioned Top Strand decreased prestress losses by marginal amounts. Using the AASHTO Refined Method, TL was reduced from 43.1 to 39.6 ksi (297 to 273 MPa). Using the Jayaseelan Time Step Method, TL was reduced from 41.6 to 38.2 ksi (287 to 263 MPa). The 3.4 to 3.5 ksi (23 to 24 MPa) reduction in TL represents less than 2% of total prestressing.
4. The inclusion of Mild Steel Reinforcement at the CGS reduced prestress losses by marginal amounts. Using the Jayaseelan Time Step Method, TL was reduced from 41.6 to 38.7 ksi (287 to 267 MPa). The 1.9 ksi (13 MPa) reduction represents less than 1% of total prestressing.

5. The inclusion of Fully Tensioned Top Strand decreased camber in prestressed beams by significant amounts. The design with four fully tensioned top strands (T4) reduced camber at 90 days (just prior to slab casting) from 4.08 to 3.44 in. (104 to 87 mm). The 0.64 in. (16 mm) reduction in camber represents 16% of the total prior to slab casting. The long term camber is reduced from 1.81 to 1.00 in. (46 to 25 mm). This 0.81 in. (21 mm) reduction in camber represents 45% of the total. The significance of this number means that long term serviceability and ride quality is more assured by using Fully Tensioned Top Strand.
6. The inclusion of Mild Steel Reinforcement at the CGS reduced camber in prestressed beams by significant amounts. The design with five #9 bars (MS 5.0) reduced camber at 90 days from 4.08 to 3.58 in. (104 to 91 mm). The 0.50 in. (13 mm) reduction in camber represents a 12% reduction in camber prior to slab casting. The long term camber is further reduced from 1.81 to 1.37 in. (46 to 35 mm) This 0.44 in. (11 mm) reduction in camber represents 24% of the total. The significance of this numbers means that long term serviceability and ride quality is more assured when using Mild Steel within the cross section of the prestressed concrete girder.
7. Combining the two prior bullet points, the Inclusion of Both Fully Tensioned Top Strands with Mild Reinforcement (T4 + MS 5.0) reduced initial camber from 2.98 in. (76 mm) to approximately 2.3 in. (58 mm). Camber at 90 days was reduced from 4.08 in. (104 mm) to approximately 2.8 in. (71 mm). This 1.3 in. (33 mm) reduction in camber at slab casting can ease construction by decreasing the height of required haunches to “make-up” elevation dissimilarities. Long-term camber is also reduced from 1.81 in. (46 mm) to approximately 0.50 in. (13 mm) This is approximately a 1.3 in. (33 mm) reduction in camber, or a 72% reduction in camber of the prestressed concrete bridge girder.
8. The inclusion of Fully Bonded Top Steel with the Mild Steel can work to reduce short term and near term cambers, marginally improve the constructability of prestressed concrete bridges, and produce as-built bridges with greater assurance of long term serviceability and ride quality.

## **RECOMMENDATIONS**

1. The AASHTO Refined Method requires modification that incorporates the inclusion of mild steel into the prestress loss equations.

## **ACKNOWLEDGMENTS**

The authors gratefully acknowledge the sole sponsor for this research, Oklahoma Department Of Transportation (ODOT).

## References

1. ACI 209R-92, A. (1992). "Prediction of Creep, Shrinkage, and Temperature Effects in Concrete Structures. ACI 209R-92, Reported by ACI Committee 209.
2. ACI Committee 318, 2014. Building Code Requirements for Structural Concrete (ACI 318-14): An ACI Standard: Commentary on Building Code Requirements for Structural Concrete (ACI 318R-14), an ACI Report, American Concrete Institute.
3. Greuel, A., B. T. Rogers, R. A. Miller, B. M. Shahrooz and T. M. Baseheart (2000). "Evaluation of a high performance concrete box girder bridge." *PCI journal* **45**(6).
4. Hale, W. M. and B. W. Russell (2006). "Effect of allowable compressive stress at release on prestress losses and on the performance of precast, prestressed concrete bridge girders." *PCI journal* **51**(2).
5. Huo, X. S., N. Al-Omaishi and M. K. Tadros (2001). "Creep, shrinkage, and modulus of elasticity of high-performance concrete." *Materials Journal* **98**(6): 440-449.
6. Lin, T. Y. and N. H. Burns (1981). "Design of prestressed concrete structures".
7. AASHTO LRFD (2014). AASHTO LRFD bridge design specifications, Washington DC: American Association of State Highway Transportation Officials.
8. PCI Design Handbook (1997). Precast/Prestressed Concrete Institute. Chicago, IL.
9. Martin, L. D. and C. J. Perry (2004). PCI design handbook: precast and prestressed concrete, Prestressed Concrete Inst.
10. Pessiki, S., M. Kaczinski and H. H. Wescott (1996). "Evaluation of effective prestress force in 28-year-old prestressed concrete bridge beams." *PCI journal* **41**(6): 78-89.
11. Preston, H. K. (1975). "Recommendations for estimating prestress losses." *PRECAST/PRESTRESSED CONCRETE INSTITUTE. JOURNAL* **20**(4).
12. Shenoy, C. V. and G. C. Frantz (1991). "Structural tests of 27-year-old prestressed concrete bridge beams." *PCI Journal* **36**(5).
13. Tadros, M. K., N. Al-Omaishi, S. Sequirant and J. Gallt (2003). "NCHRP Report 496." *Prestress Losses in Pretensioned High-Strength Concrete Bridge Girders.*
14. Tadros, M. K., A. Ghali and W. H. Dilger (1975). "Time-dependent prestress loss and deflection in prestressed concrete members." *PCi Journal* **20**(3): 86-98.
15. Tadros, M. K., A. Ghali and A. W. Meyer (1985). "Prestressed Loss and Deflection of Precast Concrete Members." *PCI Journal* **30**(1): 114-141.

## Notation

$A_g$	=	gross cross- sectional area
$A_{ps}$	=	area of prestressing strands
$A_{tr}$	=	transformed cross- sectional area
$CR$	=	loss due to Creep of Concrete
$E_{ct}$	=	modulus of Elasticity of concrete at transfer or time of load application
$E_c(t)$	=	modulus of Elasticity of concrete at time t
$E_{eff}$	=	effective modulus of elasticity of concrete
$e_g$	=	eccentricity of the prestressing strands calculated using gross cross section properties (in)
$E_{ps}$	=	modulus of elasticity of prestressing strands
$E_{ps}$	=	modulus of Elasticity of prestressing steel
$ES$	=	loss due to Elastic Shortening
$e_{tr}$	=	eccentricity of the prestressing strands calculated using transformed cross section properties
$f_b$	=	concrete stresses at bottom fiber
$f'_c$	=	concrete specified compressive strength
$(f'_c)_{28}$	=	specified 28 day compressive strength of concrete.
$f_{cds}$	=	stress in concrete at center of gravity of tendons due to all superimposed permanent dead loads
$f_{cgp}$	=	the concrete stress at the center of gravity of prestressing tendons due to the prestressing force immediately after transfer and the self weight of the member at the section of maximum moment
$f_{cir}$	=	net compressive stress in concrete at center of gravity of tendons immediately after the prestress has been applied to the concrete
$f_{cpi}$	=	stress in concrete at center of gravity of tendons due to $P_{pi}$
$f_g$	=	stress in concrete at center of gravity of tendons due to weight of structure at time of prestress is applied
$f_{pt}$	=	initial prestress in prestressing strands immediately after transfer
$f_{pu}$	=	ultimate strength of prestressing tendon
$f_{py}$	=	specified yield strength of prestressing steel
$f_t$	=	concrete stresses at the top fiber



$H$	=	relative humidity
$I_g$	=	gross moment of inertia of the section
$I_{tr}$	=	transformed moment of inertia of the section
$k_{hc}$	=	humidity factor for creep
$k_{hs}$	=	humidity factor for shrinkage
$k_s$	=	factor for the effect of the volume-to-surface ratio of the component
$K_{sh}$	=	transformed cross section coefficient that accounts for the time-dependent interaction between concrete and prestressing steel.
$k_{td}$	=	time development factor
$M_{S.W}$	=	moment due to self weight of the girder
$n_{eff}$	=	effective modular ratio
$P_{pi}$	=	initial prestressing force in the prestressing strands
$P_{pi}$	=	Prestressing force in the tendons
$RE$	=	loss due to Relaxation of Prestressing strands
$SH$	=	loss due to Shrinkage of Concrete
$t$	=	age of the concrete in days
$t$	=	maturity of concrete
$t_i$	=	age of concrete at time of load application
$V/S$	=	volume-to-surface ratio
$w$	=	unit weight of concrete
$\alpha$ and $\beta$	=	constants
$\psi(t)$	=	creep coefficient at time $t$
$\psi(t, t_i)$	=	creep coefficient
$\epsilon_{sh}(t)$	=	shrinkage strain at time $t$
$\epsilon_t$	=	concrete strains at the top fiber
$\epsilon_b$	=	concrete strains at the bottom fiber
$\Delta\epsilon_{cr}(t)$	=	incremental creep strain at time $t$

## About the authors



Hema Jayaseelan is a PhD student in the Civil and Environmental Engineering Department at Oklahoma State University, Stillwater, Oklahoma. After completing her MSCE at Oklahoma State in 2007, she worked as a Structural Engineer in Kansas City for one year and in Swansea, Wales, UK for a number of years.



Bruce W. Russell, Ph.D., P.E., F.ACI, is Director of the Bert Cooper Engineering Laboratory and an Associate Professor of Civil and Environmental Engineering at Oklahoma State University, Stillwater, Oklahoma. He has been a PCI Member since 1990, and currently serves on the PCI Technical Activities Council, the PCI Bridges Committee, the PCI Concrete Materials Committee and the PCI Committee on Fire.

## **ABSTRACT**

**This paper estimates prestress losses for a prestressed concrete bridge made with Type IV Bridge Girder spanning 103.33 ft. (31.5 m). Five methods were employed to estimate losses including both the AASHTO LRFD Approximate Method and the Refined Method. The newly developed Jayaseelan Time Step Method is presented and compared to other results. We investigated the effects on prestress losses and camber from fully tensioned top strands and also from non-prestressed mild steel. Our paper demonstrates that: (1) all five methods employed to estimate losses provided results that were within 2% of one another, (2) that both the Inclusion of Top Strand and Mild Steel have small, but beneficial effects on reducing the prestress losses and (3) that the Inclusion of Top Strand and Mild Steel reduced cambers by 70 percent in prestressed concrete bridge designs that were studied.**

### **Keywords**

Bridge, bridge girder, concrete, prestressed, losses, camber, deflection

**Table 1. Prestress Losses at mid-span calculated using Gross-Section Properties with PCI Design Hand Book Method**

Case	Concrete Age	ES	CR	SH	RE	Losses at mid-span
		(ksi)	(ksi)	(ksi)	(ksi)	(ksi)
Base	90 days	17.5	27.2	5.8	3.0	53.5
	10 years	17.5	13.3	5.8	3.5	40.1
T2	90 days	16.3	25.3	5.8	3.1	50.5
	10 years	16.3	13.0	5.8	3.6	38.7
T4	90 days	15.5	24.0	5.8	3.2	48.5
	10 years	15.5	13.2	5.8	3.6	38.1
MS.2.4	90 days	<b>Prestress Losses Same as Base Case</b>				
	10 years					
MS 5.0	90 days					
	10 years					

**Table 2. Prestress Losses at mid-span calculated using Transformed Cross-Section Properties with PCI Design Hand Book Method**

Case	Concrete Age	ES	CR	SH	RE	Losses at mid-span
		(ksi)	(ksi)	(ksi)	(ksi)	(ksi)
Base	90 days	18.2	28.2	5.8	2.9	55.1
	10 years	18.2	15.6	5.8	3.4	43.0
T2	90 days	17.0	26.4	5.8	3.0	52.2
	10 years	17.0	15.2	5.8	3.5	41.5
T4	90 days	16.3	25.2	5.8	3.1	50.3
	10 years	16.3	15.3	5.8	3.5	40.8
MS.2.4	90 days	17.6	27.2	5.8	3.0	53.5
	10 years	17.6	15.1	5.8	3.5	41.9
MS 5.0	90 days	17.0	26.3	5.8	3.0	52.1
	10 years	17.0	14.6	5.8	3.5	40.8

**Table 3. AASHTO LRFD Bridge Design Specifications (2014), Approximate Estimates of Total Losses**

Case	ES	CR+SH+RE	Losses at mid-span
	(ksi)	(ksi)	(ksi)
Base	20.2	25.6	45.8
T2	18.8	26.4	45.2
T4	17.8	27.3	45.1
MS 2.4	<b>Prestress Losses Same as Base Case</b>		
MS 5.0			

**Table 4. AASHTO LRFD Bridge Design Specifications (2014), Refined Estimates of Time-Dependent Losses at mid-span calculated using Gross Section properties**

Case	Concrete Age	ES	CR	SH	RE	Losses at mid-span
		(ksi)	(ksi)	(ksi)	(ksi)	(ksi)
Base	90 days	20.2	14.1	5.1	1.2	40.6
	10 years	20.2	13.3	7.1	2.4	43.1
T2	90 days	18.8	13.3	5.2	1.3	38.4
	10 years	18.8	12.5	7.2	2.5	41.0
T4	90 days	17.8	12.7	5.2	1.3	37.0
	10 years	17.8	12.0	7.2	2.6	39.6
MS.2.4	90 days	<b>Prestress Losses Same as Base Case</b>				
	10 years					
MS 5.0	90 days					
	10 years					

**Table 5. Jayaseelan Time Step Method, Prestress losses at mid-span**

Case	Concrete Age	ES	CR	SH	RE	Losses at mid-span
		(ksi)	(ksi)	(ksi)	(ksi)	(ksi)
Base	90 days	18.3	14.8	5.6	1.1	39.8
	10 years	18.3	13.3	7.8	2.2	41.6
T2	90 days	17.1	13.9	5.7	1.2	37.8
	10 years	17.1	12.2	7.8	2.4	39.5
T4	90 days	16.3	13.3	5.7	1.2	36.5
	10 years	16.3	11.5	7.9	2.4	38.2
MS.2.4	90 days	17.7	14.1	5.4	1.1	38.3
	10 years	17.7	12.6	7.5	2.3	40.1
MS 5.0	90 days	17.0	13.4	5.2	1.2	36.9
	10 years	17.0	12.0	7.2	2.4	38.7

**Table 6. Jayaseelan Time Step method, Camber Estimation at mid-span**

Case	Camber at 1 day after release	Camber at 90 days, prior to slab cast	Camber at 91 days after slab cast	Long Term Camber at mid-span
	(in)	(in)	(in)	(in)
Base	-2.98	-4.08	-2.17	-1.81
T2	-2.73	-3.77	-1.81	-1.42
T4	-2.48	-3.44	-1.43	-1.00
MS 2.4	-2.88	-3.84	-1.98	-1.59
MS 5.0	-2.77	-3.58	-1.78	-1.37



**Figure 1.** North Canadian River Overflow Structure, John Kilpatrick Turnpike, Oklahoma, consistently of nineteen 103'-4" spans in both northbound and southbound directions with Type IV Girders spaced at 8'-0" centers.



**Figure 2.** View underneath the North Canadian Overflow Structure. John Kilpatrick Turnpike, Oklahoma.

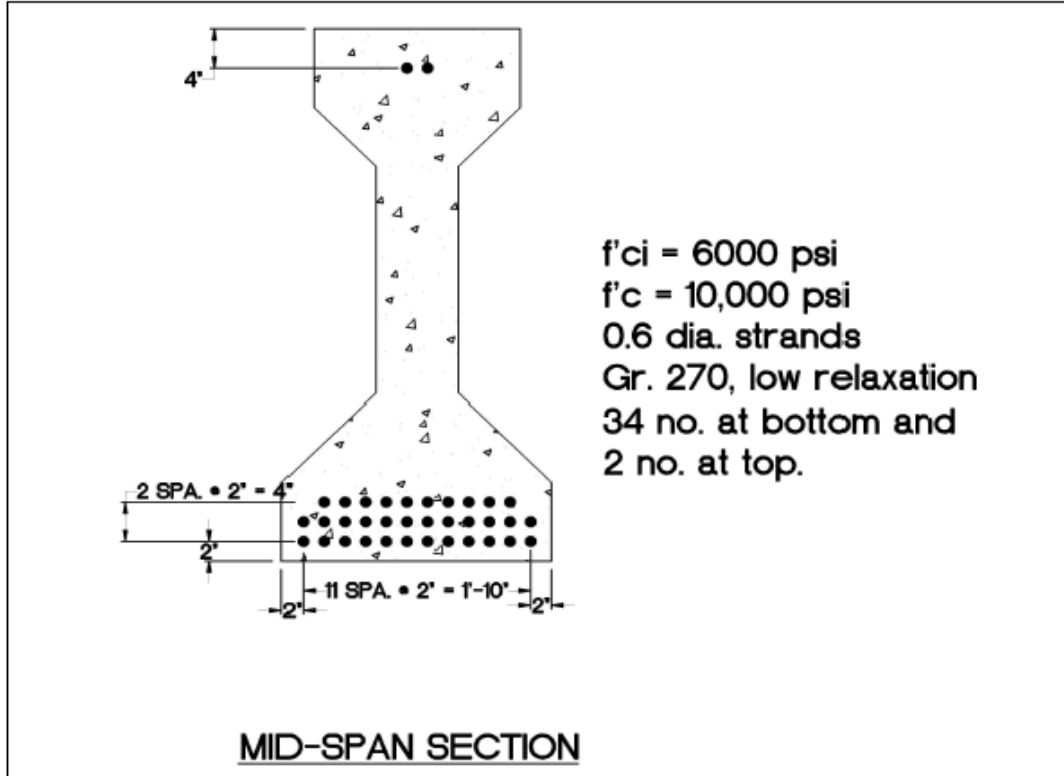


**Figure 3.** Type IV Cross Section with thirty-four (34) 0.6 in strands in the bottom flange.

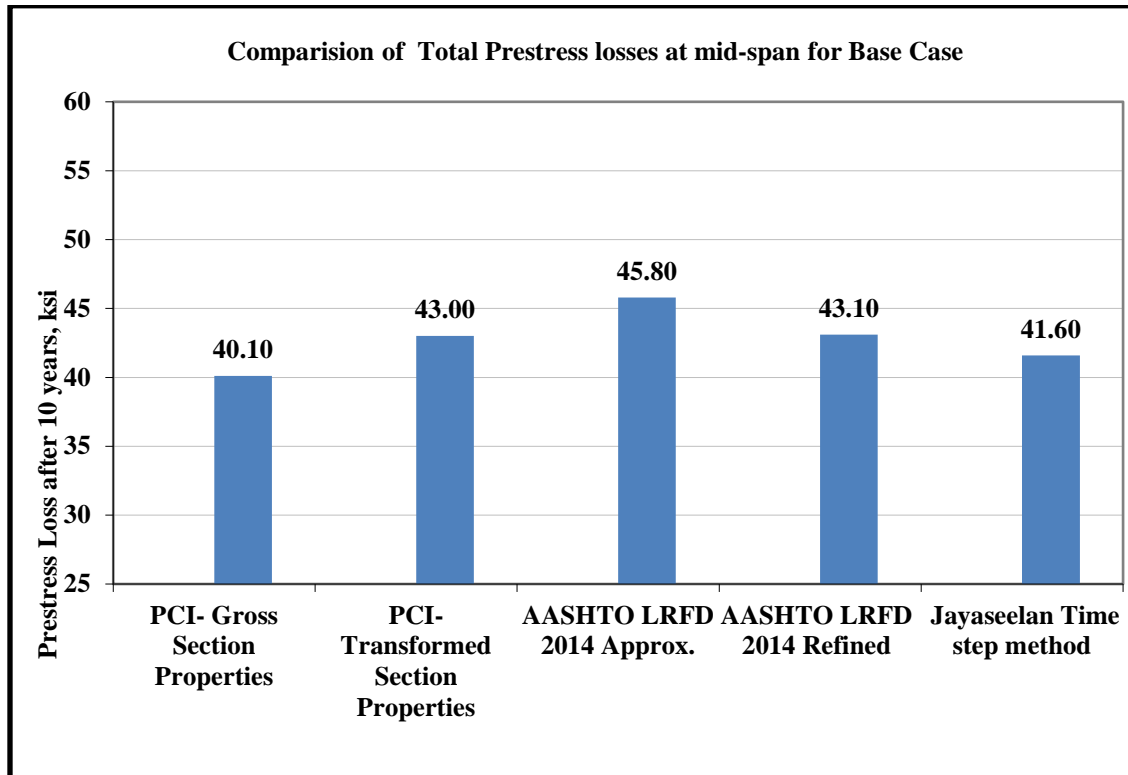


**Figure 4.** Comparison of Total Prestress Losses at mid-span for Base Case. Note: 1 ksi = 6895 kPa.



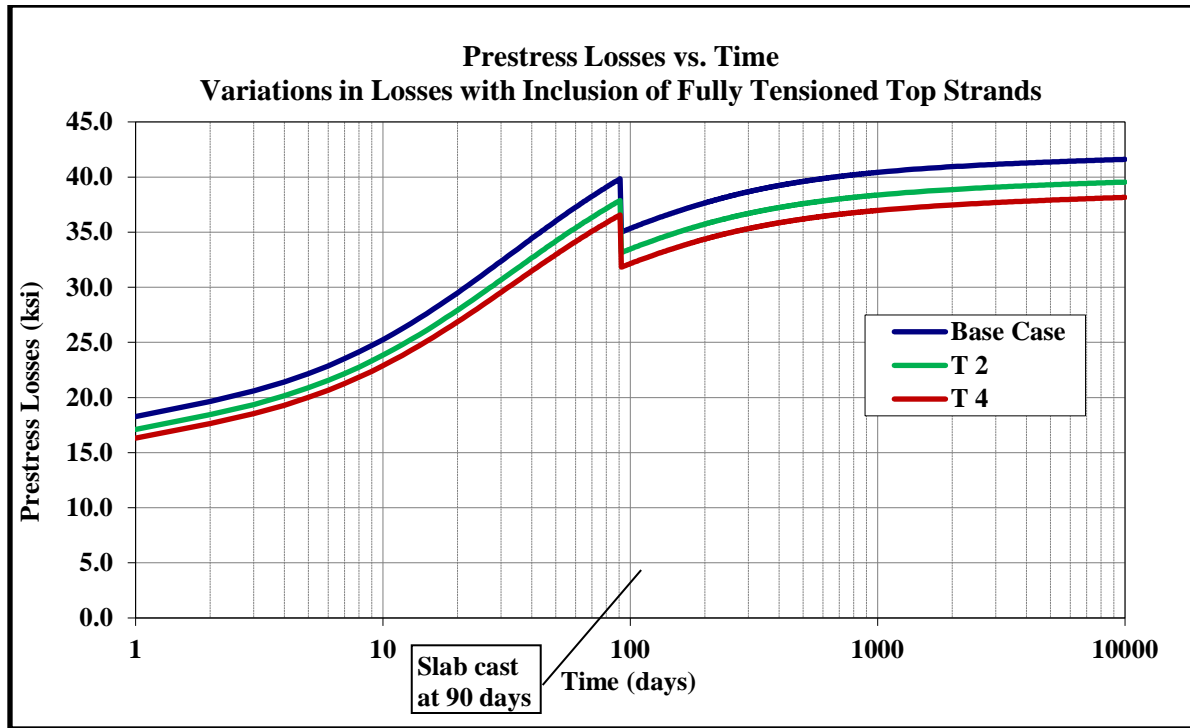


**Figure 5.** Prestress Losses vs. Time at mid-span using the Jayaseelan Time Step method. Variations in losses are charted to show variations resulting for Inclusion of Full-Tensioned Top Strands. Note: 1 ksi = 6895kPa.

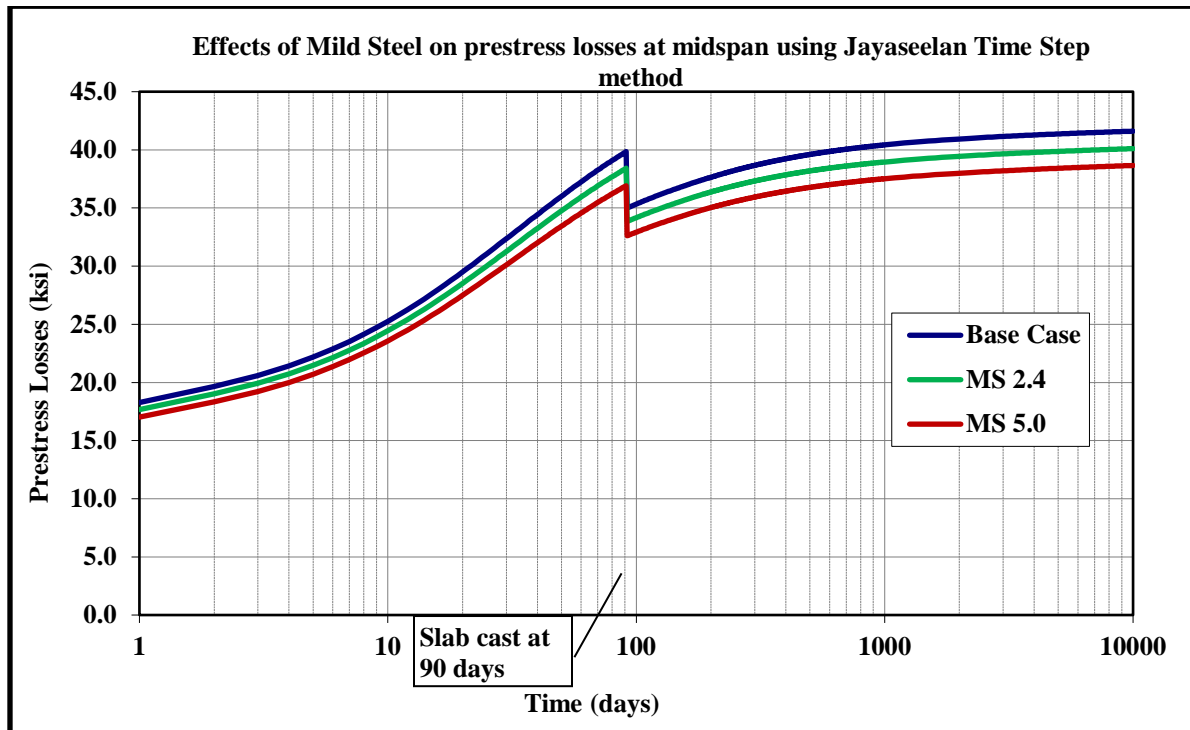


**Figure 6.** Effects of Mild Steel on Prestress Losses at mid-span using Jayaseelan Time Step method. Note: 1 ksi = 6895 kPa.

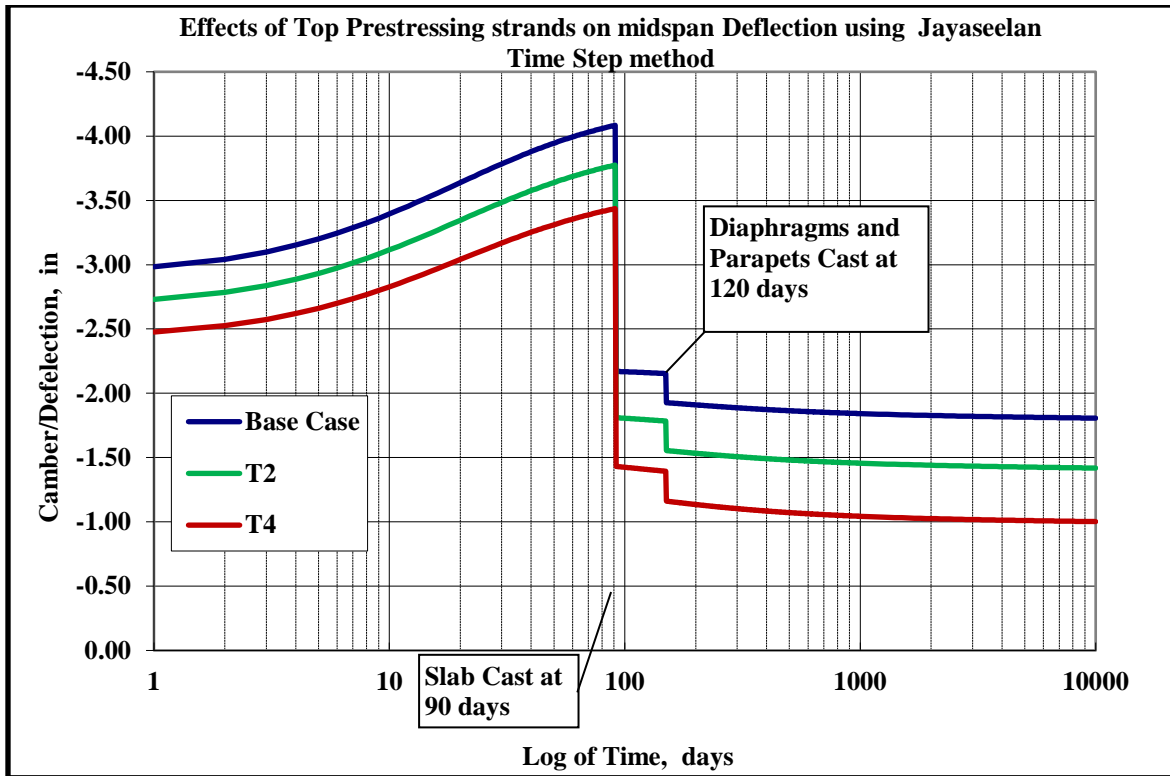


**Figure 7.** Effects of Top Prestressing Strands on mid-span deflection using Jayaseelan Time Step method.  
Note: 1 in. = 25.4 mm.

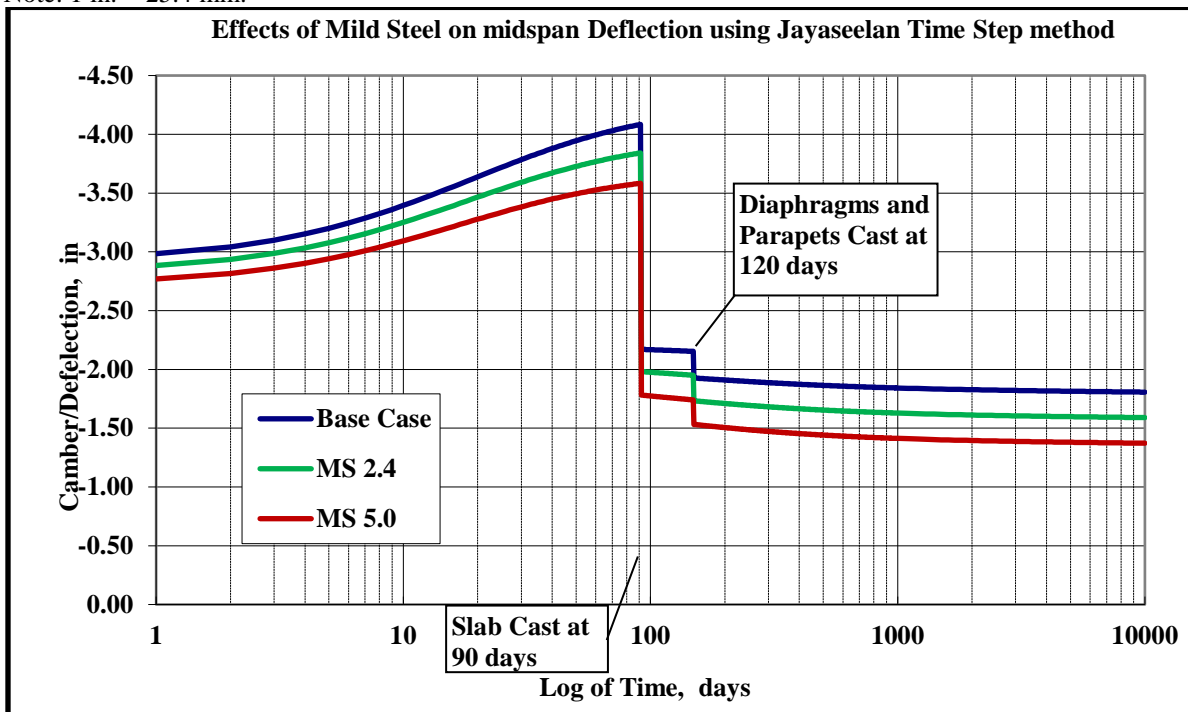


**Figure 8.** Effects of Non-prestressing steel/Mild steel on mid-span deflection using Jayaseelan Time Step method  
Note: 1 in. = 25.4 mm.

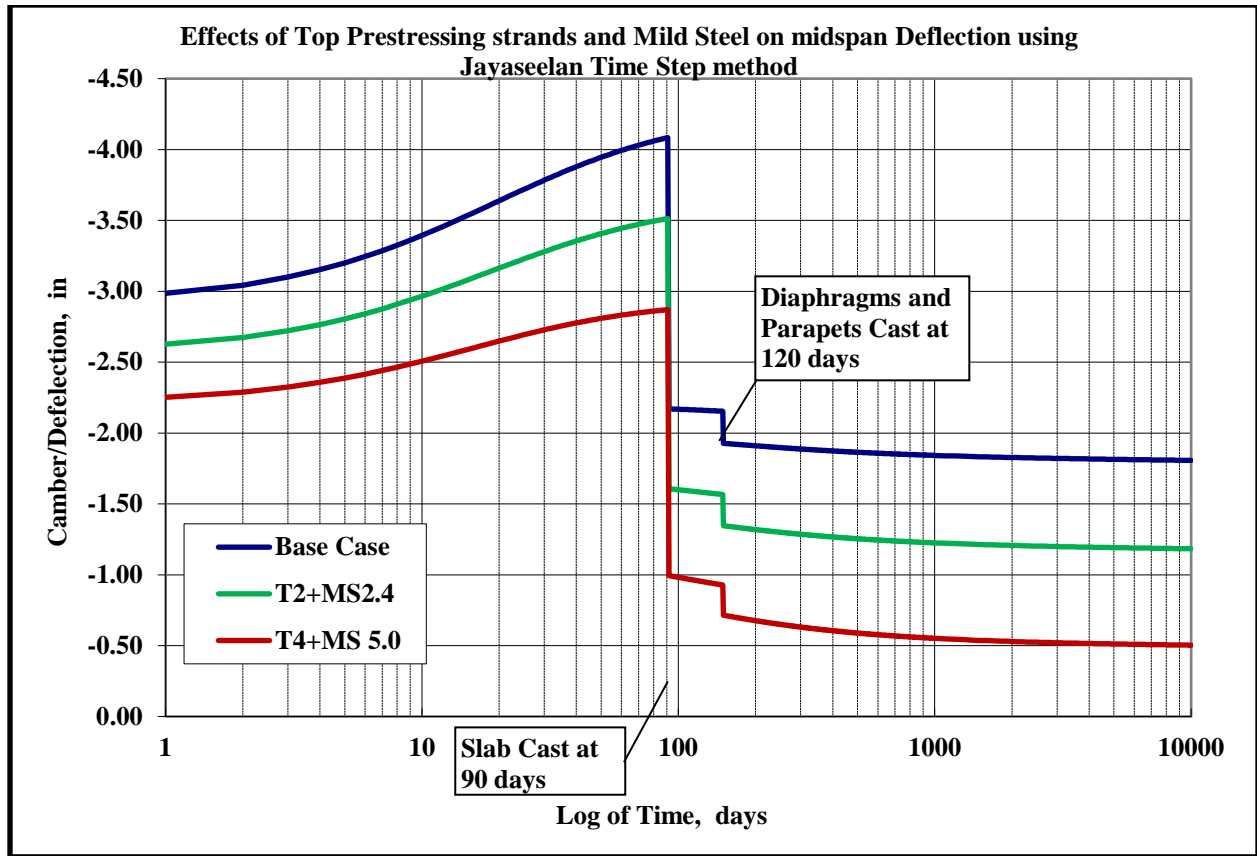


**Figure 9.** Effects of Top prestressing strands and Mild Steel on mid-span deflection using Jayaseelan Time Step method. Note: 1 in. = 25.4 mm.